ISSN 1061-933X, Colloid Journal, 2018, Vol. 80, No. 1, pp. 59–72. © Pleiades Publishing, Ltd., 2018.
Original Russian Text © S.P. Molchanov, V.I. Roldughin, I.A. Chernova-Kharaeva, G.A. Yurasik, I.N. Senchikhin, 2018, published in Kolloidnyi Zhurnal, 2018, Vol. 80, No. 1, pp. 63–77.

The Factors Determining Formation Dynamics and Structure of Ring-Shaped Deposits Resulting from Capillary Self-Assembly of Particles

S. P. Molchanov[a], V. I. Roldughin[b, *], I. A. Chernova-Kharaeva[c], G. A. Yurasik[c], and I. N. Senchikhin[b]

[a] *Topchiev Institute of Petrochemical Synthesis, Russian Academy of Sciences, Moscow, 119071 Russia*
[b] *Frumkin Institute of Physical Chemistry and Electrochemistry, Russian Academy of Sciences, Moscow, 119071 Russia*
[c] *Photochemistry Center, Russian Academy of Sciences, Moscow, 119421 Russia*
**e-mail: vroldugin@yandex.ru*

Received July 25, 2017

Abstract—The influence of different physicochemical parameters, such as particle concentration and size, droplet volume, dispersion medium composition, and substrate hydrophilicity, on the structure of deposits resulting from evaporating sessile droplets of colloidal dispersions has been studied. Parameters enabling one to targetedly control the structure of a deposit have been determined. The possibility of obtaining deposits having the shapes of thin rings and monolithic disks has been shown. The conditions have been found under which monolayer and multilayer deposits with ordered arrangement of particles are formed.

DOI: 10.1134/S1061933X18010076

1. INTRODUCTION

Capillary self-assembly is an important stage of various processes of contemporary nanotechnologies [1–3]. It is the main mechanism governing the so-called "coffee-ring effect" (CRE), which has drawn the attention of researchers after works [4, 5] were published. This effect consists in the formation of a ring-shaped structure along the perimeter of an evaporating colloidal dispersion droplet. The mechanism of deposit formation is, at first sight, rather obvious, although, possibly, hardly controlled. Numerous studies have shown that the capillary self-assembly of particles in the CRE is realized via several stages of a rather complex process, which is affected by different factors. Some of them seem to be quite predictable. They are the nature of a dispersion medium [6]; the sizes, shapes, and the state of the surface of particles [7–9]; the presence of surfactants in a system [10]; and the degree of hydrophilicity/hydrophobicity of a substrate [11–16]. Effects relevant to the heat transfer [17, 18] and the droplet-evaporation rate [1–3, 19, 20], which may be regulated by different methods, are less obvious but rather important factors. It is the diversity of the key factors that predetermines the nontrivial character of CRE manifestation.

The diversity of the formed structures and a rather subtle influence of the physicochemical characteristics of a system on them provide possibilities to widely use CRE, which is now applied not only for the improvement of jet printing and production of working circuit boards for electronic and sensor units, but also in archeology [21] and medicine [22].

This article is a continuation of the series of our previous detailed studies of the mechanism of ring-shaped deposit formation during the evaporation of colloidal dispersion droplets [23–27]. In [23], we studied the influence of different factors on initial contact angles θ_0 of droplets applied onto substrates. In particular, a relation between the contact angle and particle concentration and charge was noted. The dependence of the structure of a formed deposit on the value of the contact angle (to be more exact, the state of the surface) was briefly discussed. For example, it was noted that deposits with regular geometrical shapes could be formed only on a thoroughly treated (cleaned) surface. In addition, it was found that, in the case of microdroplets and uniform surfaces, the structure of a deposit depends on the θ_0 value more strongly than it does for evaporating macrodroplets. In the next article [24], several stages were distinguished in particle deposition that is realized under the CRE conditions, as well as changes in the character of meniscus displacement. Three scenarios of droplet evaporation were distinguished, with each of them being characterized by its own sequence of processes affecting meniscus displacement and deposit formation. Each scenario was characterized by not only a specific deposit shape, but also its own duration of meniscus pinning, character of displacement, and the value of the depinning contact angle. In [25], we studied the depen-

dence of the deposit structure on θ_0 and have found that, when it decreases, a passage from a ring-shaped to disk-shaped deposit may take place. In some systems, variations in θ_0 may cause a change in the scenario of evaporation, with the scenario becoming combined in some cases. At the same time, it has been noted that the scenario of deposit formation during dispersion droplet evaporation is, to a large extent, governed by the nature of particles and, only in the second place, the properties of a substrate and the value of θ_0. Works [26, 27] were devoted to studying the mechanisms of pinning and depinning of evaporating droplet meniscus, respectively. In [26], the effects of dispersion particle concentration and the degree of substrate hydrophilicity (hydrophobicity) on pinning were determined. It has been shown that there are three main mechanisms of pinning, with the first, second, and third of them being predetermined by the hysteresis of the contact angle, the adhesion of particles to a substrate, and the formation of a dense adsorption layer of particles on it, respectively. A relation between a pinning mechanism being realized and the degree of substrate hydrophilicity has been found. The data obtained in [27]have made it possible to reveal three fundamental factors responsible for depinning. The first factor is related to the hysteresis of a dispersion droplet contact angle, the second one is predetermined by the effect of particles on the dispersion surface tension, and the third factor is associated with the formation of a dense gel in the meniscus region where the dispersion medium intensely evaporates. The relation between the realized depinning mechanisms and the scenarios of droplet evaporation has been determined.

It may be said that our previous studies were focused on studying certain stages of droplet evaporation and ring-shaped deposit formation. At the same time, namely the structure and properties of a deposit are of practical interest. These characteristics were implicitly "factored out" in our previous works. Only the diversity of the formed structures was noted, and, in [25], their relation to the initial contact angle was monitored in a rather simple situation. The dynamics of deposit formation was not studied in detail. Pinning and depinning, which have been studied in [26, 27], are just important separate stages of this dynamics. Thus, the dynamics of the capillary self-assembly and the possibilities of the control over self-organizing structures remain, in some sense, being uninvestigated.

In this work, we shall analyze the role of a number of factors (in addition to θ_0) namely in the formation of ring-shaped deposits. The relation will be determined between the final structure of a deposit and the dynamics of its formation. We intend to comprehensively consider the effect of the initial particle concentration in a solution, droplet size, dispersion-medium composition, and substrate wettability on the structure resulting from the capillary self-assembly of particles.

2. EXPERIMENTAL

Experiments were performed with dispersions of polystyrene latex particles with diameters $d_p = 86$, 200, 240, 250, and 540 nm [28] and silica particles with $d_p = 225$, 250, and 255 nm obtained by tetraethoxysilane hydrolysis in ethanol in the presence of ammonia as a catalyst [29]. Polystyrene particles contained NH^- and CO^- surface groups in a concentration of 2×10^{-6} mol/m^2.

Particle sizes were determined by dynamic light scattering with a Photocor Complex spectrometer (Fotocor Ltd, Russia).

Particles were dispersed in deionized water obtained by sorption and ion-exchange filtration followed by mechanical microfiltration in a D-301 deionizer (Akvilon, Russian Federation). In addition, dimethyl sulfoxide (DMSO), ethanol, and ethylene glycol were used as components of dispersion media.

Thermo Scientific SuperFrost cover glasses (CGs) (Menzel-Glaser, Germavy) with sizes of $76 \times 26 \times 1$ mm^3 preliminarily cleaned from contaminants were used as substrates. All CGs were cleaned in the same manner as follows:

(1) initially, they were washed with tap water and, then, with distilled water to remove main contaminants;

(2) they were placed into a glass beaker and successively treated with a Fairy detergent solution, acetone, and chromic mixture in an ultrasonic bath for 10–20 min;

(3) they were washed with deionized water and dried.

Before the experiments on droplet evaporation, the dispersions were treated in a 2.8-L UZV-2 ultrasonic bath (NPP Sapfir, Russian Federation) for 15 min.

Microdroplets were applied onto the substrates using a Lenpipet Digital one-channel dosing pipette equipped with replaceable heads, which enabled us to obtain droplets with volumes of 10–100 μL.

In addition, CGs coated with a polystyrene film (500 nm thick) with a Spincoater P6700 (Specialty Coating Systems, United States) were used as hydrophobic substrates. The films were formed in the following way. Initially, a saturated polystyrene solution in toluene was prepared. For this purpose, polystyrene (0.1 g) and toluene (0.8 mL) were placed into an Eppendorf tube, which was exposed in a thermoshaker for 60 min (1400 rpm, 50°C). Then, the polymer solution (100 μL) was applied onto cleaned CGs with the Spincoater P6700 setup at 2000 rpm for 1 min.

Picoliter droplets were applied using a Jetlab II setup (MicroFab Inc., United States). The generated microdroplets had the following parameters: velocity

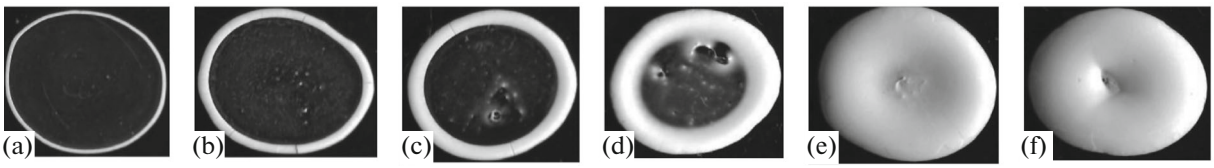

Fig. 1. Structures of deposits resulting from evaporating droplets of SiO_2 dispersions in deionized water with a particle size of 225 μm and concentrations of (a) 1, (b) 5, (c) 10, (d) 20, (e) 40, and (f) 50 wt %.

at the nozzle outlet of 2.3 ± 0.2 m/s, volume of 230 ± 25 pL, diameter of 78 ± 2 μm, and angle of deviation from the vertical of no larger than 1°.

Microdroplets were monitored using video cameras of the Jetlab II setup, a D-Eclipse C1 confocal laser scanning microscope (Nikon, Japan), and a Solver Bio scanning atomic force microscope (ASM) (NT-MDT, Russian Federation).

Macrodroplets were observed and their contact angles were measured with the help of an optical video stand (Photochemistry Center, Russian Academy of Sciences, Russia) [30] consisting of a measuring table for a substrate onto which a droplet was applied, as well as vertical and horizontal long-focus microscopes equipped with video cameras, which monitored the droplets at different angles. Before droplets were applied, a substrate was placed onto the measuring table. Then, the images were begun to be recorded (the top and side views) with preset time intervals. After that, a droplet of a specified volume was applied onto the substrate. The droplet images were taken until it was completely evaporated. The obtained images were used to determine all necessary parameters, i.e., the initial and current contact angles, as well as the angle and time of depinning. A software (Photochemistry Center, Russian Academy of Sciences, Russia) that made it possible to determine the contact angle of a droplet from the parameters of its side-view image was employed.

All experiments were performed under standard laboratory conditions: the temperature of the solutions, substrates, and environment was 20°C, and the relative humidity was 25%.

3. MECHANICAL FACTORS

It is reasonable to begin with the consideration of purely mechanical factors, such as particle concentration and size and droplet volume. Initially, we shall discuss the effect of particle concentration, because it seems to be the most natural and having an expectable character.

3.1. Particle Concentration

First, experiments were performed with dispersions of 225-μm silica particles in deionized water, with the particle concentration being varied in within a range of 1–50 wt %. Droplets with a volume of 8 μL were applied with a dosing pipette onto a cleaned CG (contact angle of 30°) located on the video stand. Droplet images were recorded (top and side views) with intervals of 2 s. A sample of the images taken from deposits (top view) is depicted in Fig. 1.

The visual observation shows that the scenario of droplet evaporation was the same in all cases: a droplet evaporated "from the periphery to the center." As the particle concentration increased, the height and width of the ring-shaped deposit grew, while its shape remained almost unchanged.

The data presented indicate that variations in the particle concentration affect the structure of the formed deposit in the predictable manner. This especially concerns dispersions of silica particles with sizes of several hundred nanometers, the behavior of which, as has previously been shown [23–27], remains actually unchanged upon slight variations in other parameters of the system. Figure 1 shows that, as the particle concentration increases, the ring thickness naturally grows. Therewith, almost all particles are deposited in the meniscus region. It can be clearly seen that, at concentrations below nearly 30 wt %, the particles are not deposited in any noticeable amount in the central region of the contact spot. The central region is covered uniformly beginning from the external (main) ring. Only at a high dispersion concentration, the particles begin to cover the central region of the contact spot. This indicates that the behavior of evaporating droplets is similar at all examined concentrations of SiO_2 dispersions. That is, in accordance with the classical scheme, the particles are delivered by compensatory flows to the region of the meniscus, which already moves over the deposit, to which they are anchored via this or that mechanism.

To some extent, the aforementioned concerns polystyrene particles, for which similar results have been obtained (Fig. 2). Recall that droplets of polystyrene dispersions evaporate "from the center to the periphery" [24]. Figure 2 illustrates the ring-shaped deposits resulting from the evaporating dispersions of 200-nm polystyrene particles on a CG (water contact angle of 30°). Droplet volume is 20 μL. Although droplet volume affects the deposit shape (see below), it may be said that, in the case under consideration, the situation is identical to that observed for the dispersion of silica particles.

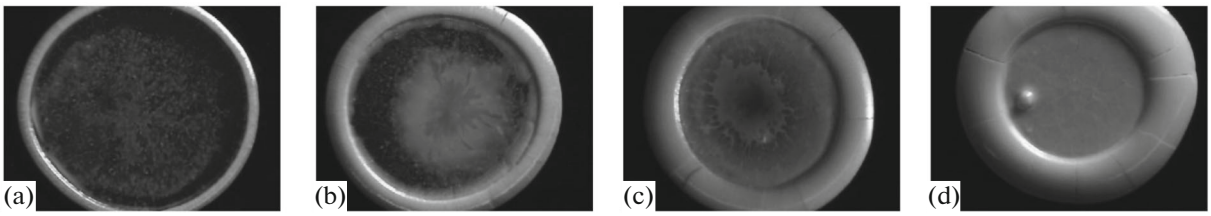

Fig. 2. Structures of deposits resulting from evaporating droplets of polystyrene dispersions with a particle size of 200 nm and concentrations of (a) 1, (b) 5, (c) 10, and (d) 20 wt %.

3.2. Particle Size

In order to exclude the influence of secondary factors, we, in this series of experiments, considered the behavior of dispersion droplets with a rather low particle concentration. Dispersions of polystyrene particles with a concentration of 1 wt % and sizes of 86, 250, or 540 nm were studied using droplets with volumes of 280 pL and 10 μL. In addition, this enabled us to partly monitor the effect of droplet size on the deposit structure.

Microdroplets with a volume of 280 pL were applied onto a hydrophilic substrate (CG with a water contact angle of 30°) using the Jetlab II setup. After droplet evaporation, the deposits formed on the substrate were studied with optical and atomic force microscopes.

Macrodroplets of a colloidal solution with the same composition and a volume of 10 μL were applied onto identical substrates with the dosing pipette. The deposits resulting from droplet evaporation were examined on the video stand; their micrographs are depicted in Fig. 3. It can be seen that both the particle size and microdroplet volume only slightly affect the deposit structure. In all cases, we have ring-shaped structures diameters of which are presented in Table 1. Therewith, the thickness of a formed ring is practically independent of the particle size. Particles are not deposited in the central region of the contact spot; i.e, they are completely transferred to the region of the main ring while droplets of all dispersions evaporate with the exception of the dispersion containing the largest particles.

The above-presented data show that the size of a ring-shaped deposit is almost independent of particle diameter in the case of macrodroplets and exhibit a nonmonotonic behavior in the case of microdroplets. Possibly, the nonmonotony observed in the behavior of the deposit diameter as a function of particle size results from the action of oppositely directed factors, i.e., the effect of particles on the surface tension (the smallest particles have the strongest effect, because, at the same weight concentration of a dispersed phase, the particle number concentrations, which govern the change in the surface tension, appear to be substantially different) and the rate of particle deposition onto the substrate. Polystyrene particles increase the surface tension [27]; therefore a larger contact angle and, accordingly, a smaller diameter of the contact spot must correspond to a smaller particle size. Hence, when passing from the dispersion of 86-nm particles to the dispersion of 250-nm particles, the diameter of the contact spot (and the ring-shaped deposit) must increase. The decrease in the diameter for particles with d_p = 540 nm seems to be related to the fact that, for this dispersion, the effect of the increase in the surface tension is weaker (particle concentration is low), while the time of particle anchoring on the substrate may increase, so that the droplets noticeably lose their volume due to the evaporation before the onset of pinning. That is, in this case, before meniscus is fixed, microdroplets have time to substantially reduce their sizes.

Table 1. Spot diameters of microdroplets d_n and macrodroplets d_m as depending on polystyrene-particle diameter d_p

d_p, nm	86	250	540
d_n, μm	114	121	90
d_m, mm	7.0	6.8	7.1

It should also be noted that some fraction of large particles remains inside of the ring-shaped deposit, with the uniformity of the deposit distribution being deteriorated with a rise in the particle size. This also indicates that they are slower anchored to the substrate.

Note that the radial distribution of the mass concentration of particles on a substrate in the central region of a contact spot is independent of the particle size (within the studied range). The apparent difference in the brightness of the deposits in Fig. 3 (especially in the central region) is due to the difference in focusing of the microscope. In addition, it is worth noting that the image brightness will be substantially different at the same weight content of particles with different sizes on a substrate: large particles scatter light many times more intensely than small particles do. This fact must be taken into account when visually analyzing the deposits that do not form monolithic uniform layers.

The insignificant variation in the sizes of the ring-shaped deposits in the case of macrodroplets is related

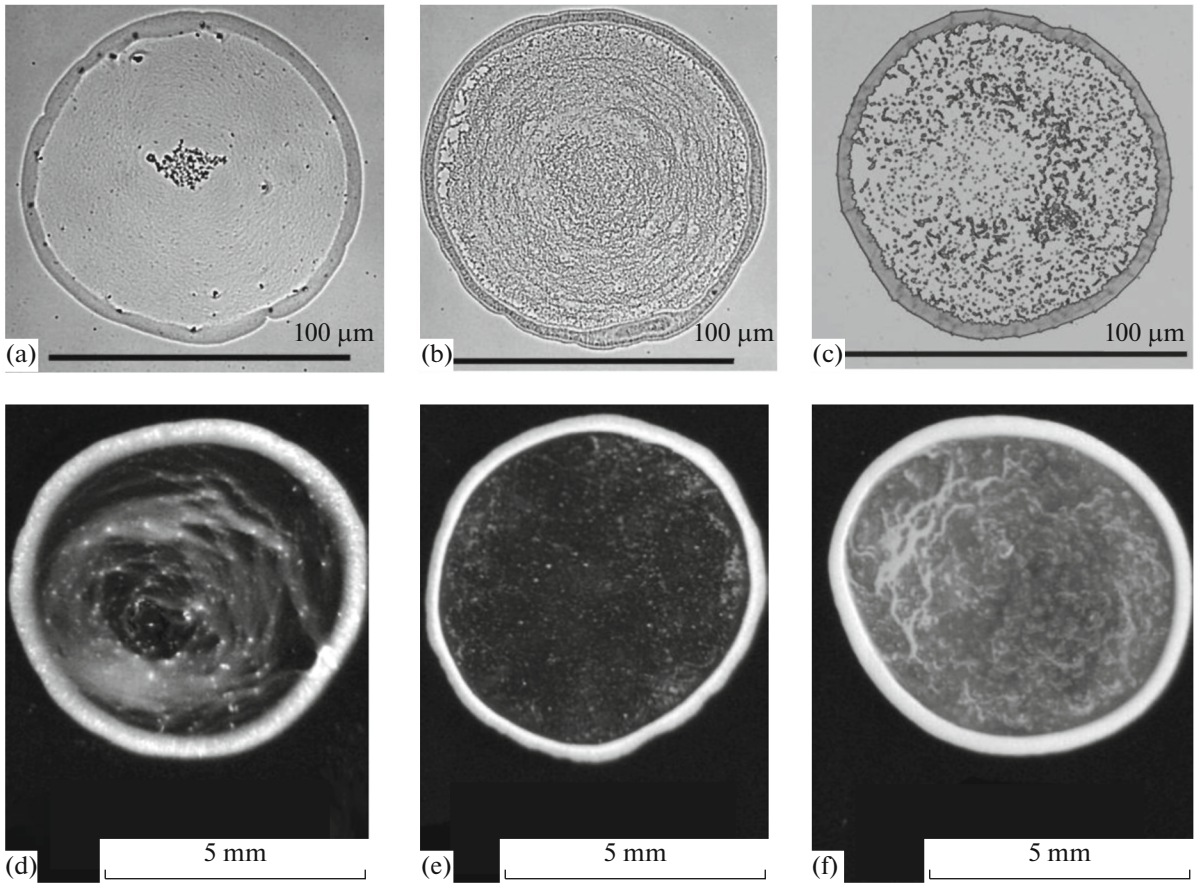

Fig. 3. Structures of ring-shaped deposits resulting from evaporating droplets of 1 wt % polystyrene dispersions: droplet volumes are (a)–(c) 280 pL and (d)–(f) 10 μL; particle sizes are (a, d) 86, (b, e) 250, and (c, f) 540 nm.

to a lower rate of a decrease in their size upon evaporation, during which, the large particles also have time to be anchored to the substrate in the meniscus region.

3.3. Droplet Volume

As we have shown above, the structure of a deposit remains unchanged upon the passage from micro- to macrodroplets. However, the situation somewhat changes for droplets of an intermediate size. Substantial differences may be observed in this case. We have carried out a series of experiments with droplets of polystyrene dispersions with a particle size of 540 nm and a concentration of 1 wt % to study the regularities of variations in deposit structure with droplet sizes.

In this series of experiments, 1, 4, 16, 32, 64, 128, 256, 512, or 999 300-pL droplets were successively applied onto selected point regions of a CG surface (water contact angle of 30°) with the Jetlab II setup at a frequency of 1000 Hz (the rate of the application was substantially higher than the rate of droplet evaporation). In this way, 9 droplets with volumes of 0.3, 1.2, 5, 10, 20, 40, 80, 160, and 300 nL were formed. The ring-shaped deposits resulting from the evaporation of these droplets were studied with optical and atomic force microscopes.

The geometric characteristics of the obtained ring-shaped deposits are listed in Table 2. The data presented in Table 2 show some proportionality between the sizes of the droplets and the ring shaped deposits. There are no marked deviations from the corresponding proportionality. However, in contrast to the geometric characteristics, the structure of the deposits undergoes substantial transformations, which can be seen in the three images depicted in Fig. 4. We have determined the structures resulting from the evaporation of all droplets applied onto the substrate. They are not presented in the figure, because the deposit structure varies gradually with the successive passages from the droplets of one size to the droplets of another size of those shown in the figure.

These data testify that the sizes of the contact spots obviously increase with droplet volume. At the same time, the shape of a deposit remains unchanged. As the droplet volume grows, the density of substrate coverage with particles increases inside of a ring (at an unchanged ratio between its width and diameter). At a droplet volume above 40 nL, small uniform “spots”

Table 2. Sizes of ring-shaped deposits as depending on volume V of microdroplets of polystyrene dispersion with a particle size of 540 nm and a concentration of 1 wt %

V, nL	0.3	1.2	5	10	20	40	80	160	300
d_n, μm	102	122	163	213	262	326	508	562	867
d_n/V, μm/nL	340	102	32.6	23.3	13.1	8.9	6.4	3.5	2.9

begin to be formed on the substrate inside of the rings; then, they grow into large zones of deposited particles. The AFM studies have shown that these "spots" are densely packed layers of particles. As the droplet volume increases, these zones widen; however, they do not fill the entire area inside of a ring, but rather multilayer structures are formed.

Since the experiments were performed with microdroplets, the dynamics of evaporation could not be monitored. On the basis of the nature of particles (polystyrene) and the available data, the evaporation in the regime "from the center to the periphery" could be expected. The increase in the amount of particles deposited in the central region with the droplet size leads us to assume the onset of the formation of a second ring. The formation of the second ring during the evaporation "from the center to the periphery" takes place in the combined regime described in [25]. That is, at a certain stage of particle deposition by the CRE mechanism, the evaporation regime changes.

However, in contrast to the situation considered in [24], the second ring-shaped deposit in the central region has not time to be formed because of the small size of the droplets. As the droplet size increases and the particle concentration in a dispersion noticeably grows at the final stage, the concentration of particles necessary for the formation of the internal deposit is reached, and a dense internal structure composed of several layers of particles is formed.

Figure 5 shows the AFM images of structure fragments located at different sites of a deposit for a 300-nL droplet. The presented data indicate that ordered structures are formed at different stages of evaporation and in different regions of the deposit. An important fact is worth noting: the thicker the deposit layer, the smaller number of defects observed in an ordered packing of particles. This is easily seen from the comparison of regions *2*–*5*, which contain different (increasing) numbers of layers of deposited particles. Indeed, the existence of region *2* in Fig. 4c directly indicates a large number of "defects" in the region with a low content of particles.

The dominant role of capillary forces in the formation of ordered structures at the final stage of evaporation has been revealed rather long ago [1]. In our case, the particles may also be ordered due to the hydrodynamic forces that press particles to the surface of evaporation. It is possible that the existence of several mechanisms of ordering leads to different packings of particles in deposits. The capillary forces begin to manifest themselves when particles "emerge" at a liquid/gas interface, and liquid isthmuses are formed between them. In the systems under consideration, the particles can emerge at the surface only in the region of a ring being formed, and, at the final stage, upon their deposition in the central region of a contact spot. The formation of ordered structures implies that the particle coagulation is slow and occurs already under the action of capillary forces. This is also evident from the existence of region *2* in Fig. 4c, which is almost free of particles and their aggregates. The presence of a small amount of individual particles and small aggregates in region *2* is, most probably, due to accidental factors, including deposition of particles onto the substrate directly from the liquid phase. As a whole, it may be believed that many particles are delivered to the region of intense evaporation, where they form the gel mentioned in [27], with this gel subsequently forming the ordered structures.

4. ROLE OF SUBSTRATE

In this section, we shall consider the role of a substrate in the formation of ring-shaped structures. In

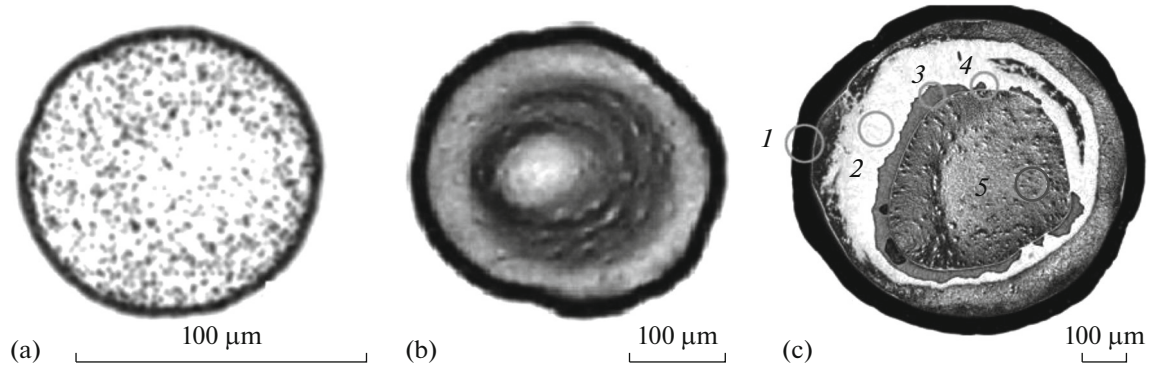

Fig. 4. Structures of deposits resulting from evaporating microdroplets of polystyrene dispersions with a particle size of 540 nm and a concentration of 1 wt %; droplet volumes are (a) 0.3, (b) 40, and (c) 300 nL.

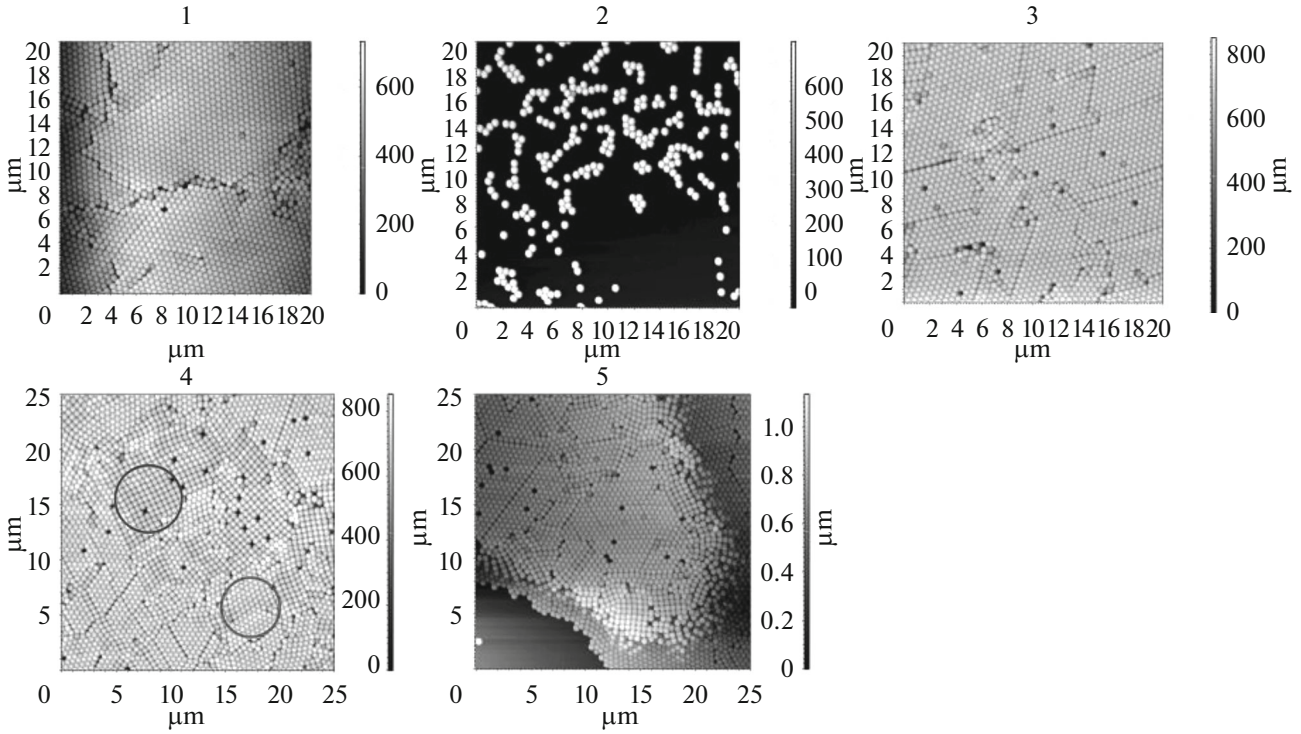

Fig. 5. AFM images of the microstructure of the solid residue presented in Fig. 4c (their numbering corresponds to the numbering of regions in Fig. 4c). The circles in image 4 denote regions in which particles have different ordered packings, i.e., square and hexagonal ones.

previous works [23–27], we have noted the important role of the degree of hydrophilicity of a substrate in the manifestation of the main effects accompanying CRE. Here, we shall focus the main attention on the effect of this factor on the structure of the formed rings.

In the experiments with hydrophilic and hydrophobic substrates, colloidal solutions of polystyrene microspheres with a diameter of 540 nm and concentrations of 0.25, 0.5, 1, 2.5, 5, and 10 wt % were used. Colloidal solution microdroplets with a volume of 280 pL were applied with the Jetlab II setup onto CGs (hydrophilic surface with a water contact angle of 30°) and CGs coated with a polystyrene layer (hydrophobic surface with a water contact angle of 85°). The structures resulting from droplet evaporation were examined with optical and atomic force microscopes. The AFM data were used to determine the particle density (deposit height) on a substrate as depending on the distance from the center of a contact spot.

The experiments were also carried out with 10-μL macrodroplets of the same colloidal solution, which were applied onto the same substrates with the help of the laboratory dosing pipette. The structure of the resulting ring-shaped deposits with larger sizes was examined on the video stand.

4.1. Hydrophilic Substrate

On a hydrophilic substrate, a meniscus is anchored immediately after a droplet is applied and its equilibrium shape is established [23–27]. The diameters of a solid deposit and an initial contact spot coincide with each other (Table 3). The data presented in Table 3 indicate that, as particle concentration increases, the diameter of the ring-shaped deposit decreases. This may be explained by a rise in the solution surface tension (see [27]), with this rise predetermining a larger contact angle and, hence, a smaller diameter of a contact spot.

Table 3. Diameters of ring-shaped deposits as depending on particle concentration C for micro- and macrodroplets of dispersions evaporating on hydrophilic and hydrophobic substrates

C, wt %	0.25	0.5	1.0	2.5	5.0	10.0
Hydrophilic substrate						
d_n, μm	190	192	185	178	170	161
d_m, mm	6.8	6.6	6.7	6.9	6.8	6.7
Hydrophobic substrate						
d_n, μm	9	14	18	23	30	37
d_m, mm	0.6	0.9	1.2	1.6	2.1	2.6

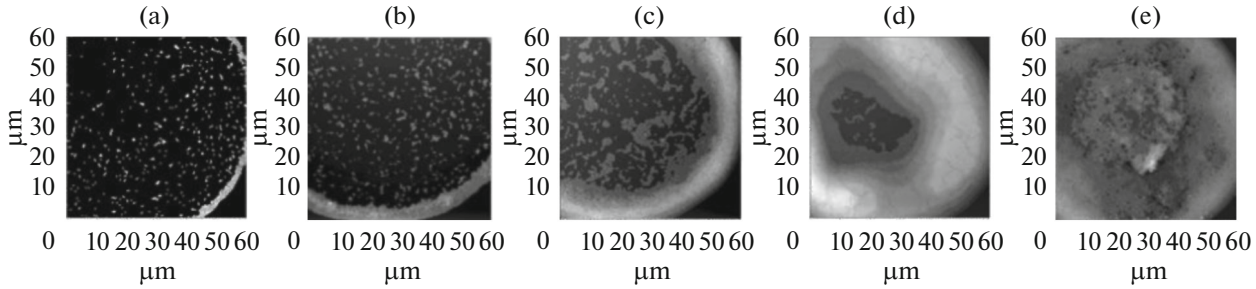

Fig. 6. AFM images of the ring-shaped structures resulting from evaporating microdroplets of polystyrene dispersions on a hydrophilic substrate: particle concentrations are (a) 0.5, (b) 1, (c) 2.5, (d) 5, and (e) 10 wt %.

Figure 6 illustrates the structures of the ring-shaped deposits resulting from evaporating microdroplets of polystyrene dispersions with different particle concentrations. Since the microdroplet volume is the same, the series of the structures corresponding to increasing concentration may, under some assumptions, be considered as the monitoring of solid deposit formation in time during evaporation of droplets with the highest particle concentration (the data on the droplets with a concentration of 0.25 wt % are not presented, because the corresponding deposit is a very thin ring resembling that presented in Fig. 6a).

The images depicted in Figs. 6a and 6b show that particles uniformly fill the space inside of the ring. That is, particles are adsorbed on the substrate beginning from the moment of droplet application. Accordingly, the longer the evaporation time, the larger amount of particles are anchored to the substrate. Further, the self-assembly of the particles in the meniscus overlaps with this process (this is confirmed by the disagreement between the structures in the central region of the contact spot and in the ring-shaped deposit). After a while, the coverage of the substrate becomes nonuniform, which may be related to the aggregation of particles transferred by lateral flows with the particles that are already located on the substrate or to their deposition at the final stage of droplet evaporation. The latter assumption is supported by the existence of a zone almost free of particles, with this zone being observed in the image of the deposit resulting from the evaporation of a dispersion droplet with a particle concentration of 5 wt %.

As has been mentioned previously [26], after a droplet has been applied onto a hydrophilic surface and its equilibrium shape has been established, meniscus pinning takes place due to the contact angle hysteresis and anchoring the meniscus to the particles deposited onto the substrate near the three-phase contact line. Pinning facilitates the development of the compensatory flows, which transfer particles from the droplet bulk to the three-phase contact line, thereby forming a "thick" peripheral ring.

Analogous results are presented in Table 3 and Fig. 7 for 10-μL macrodroplets. Note that, in contrast to microdroplets, the diameter of the solid deposit resulting from the evaporation of macrodroplets does not decrease with an increase in the particle concentration. Within the error caused by possible fluctuations in the sizes of a droplet/substrate contact spot associated with, in particular, the manual application of macrodroplets, the size of a formed ring may be considered to be independent of particle concentration. Possibly, this is due to the fact that at this technique of the application of rather large droplets, they initially "spread" to a certain size of the contact spots because of inertia effects; then, their constant sizes are established due to the contact angle hysteresis.

The data presented in Fig. 7 show that, even at the lowest concentration of particles, when the peripheral ring is not formed because of their deficiency, the whole substrate surface under a droplet is almost entirely covered with particles. The small difference between the heights (the height of the ring almost coincides with that of accidentally formed clusters of particles, see the scale of the ordinate axis) resembles noticeable substrate asperities, which, as can be seen in the profile, are absent.

It should be noted that, as the droplet volume increases, the fraction of particles deposited in the central region of the contact spot markedly increases. This testifies that the similarity of the structures resulting from evaporating micro- and macrodroplets may be distorted. The distortion of the similarity is caused by different times and rates of the evaporation of micro- and macrodroplets. Microdroplets evaporate nearly 1000 times faster. The higher evaporation rate of microdroplets provides more intense delivery of particles to the meniscus region by the compensatory flows. Macrodroplets evaporate slower and longer; therefore, substantial amounts of particles have time to be deposited in the central region of the contact spot (see Fig. 7), thereby resulting in a substantially smaller relative width of the ring-shaped deposit. As the particle concentration increases, the ring width and the density of the layer of particles deposited in the central region of the contact spot naturally grow. As a whole, the formed structures correspond to the simplest

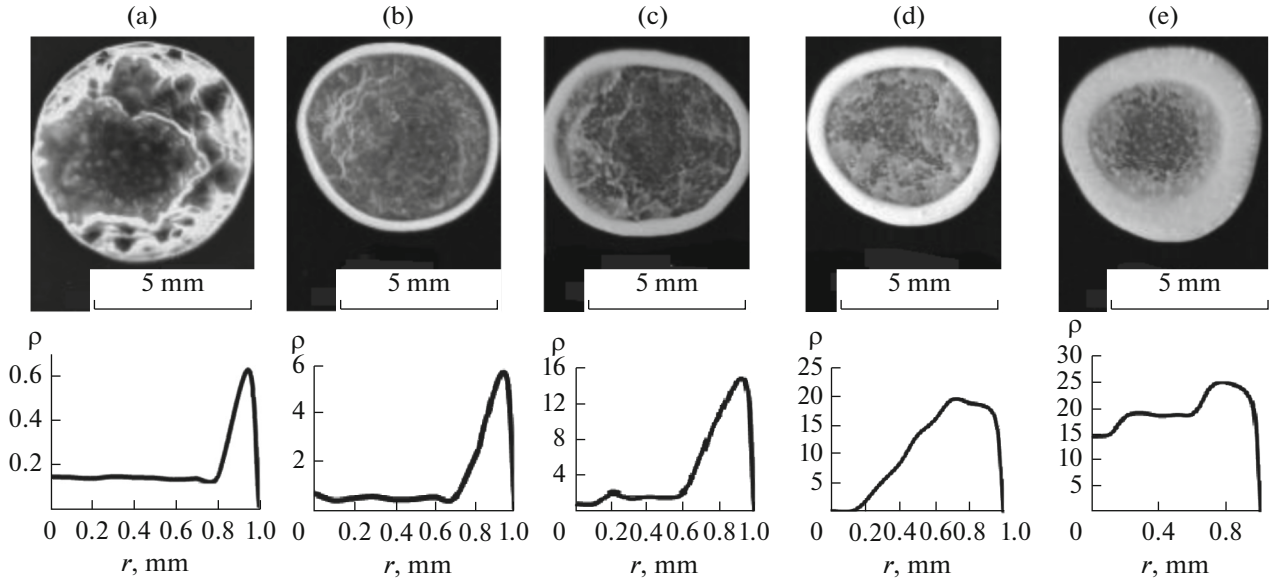

Fig. 7. Optical photographs of ring-shaped deposits formed on a hydrophilic substrate from macrodroplets of polystyrene dispersions with particle concentrations of (a) 0.25, (b) 1, (c) 2.5, (d) 5, and (e) 10 wt % and corresponding radial profiles of particle concentrations ρ (particle number/μm^2) (below) obtained with the help of video stand.

scheme of deposit formation under the CRE conditions.

4.2. Hydrophobic Substrate

On a hydrophobic substrate [26], in contrast to a hydrophilic one, meniscus is anchored some time after a droplet is applied and its equilibrium shape is established. Before the pinning onset, a droplet evaporates in the regime "at an unchanged shape." Table 3 presents the data on the diameters of the deposits resulting from evaporating microdroplets of dispersions with different particle concentrations. The data indicate that an increase in the particle concentration in a solution leads to a substantial increase in deposit diameter. The increase in the deposit diameter obviously follows from the mechanism of meniscus anchoring on a hydrophobic surface [26], which takes place when a certain concentration of particles in a solution has been reached and their dense adsorption layer has been formed. In the case of dispersions with high initial particle concentrations, the critical concentration ensuring pinning onset is reached at earlier stages of droplet evaporation.

We failed to characterize the shapes of the surfaces of all deposits resulting from evaporating microdroplets by both optical and AFM methods. On the basis of general considerations (see also [26]), it may be assumed that the deposit has the shape of a ball segment (see below).

The optical images of the deposits resulting from evaporating macrodroplets are depicted in Fig. 8, while the deposit diameters are presented in Table 3. Figure 8 shows that, in the case of a low particle concentration, when pinning occurs after a substantial decrease in droplet sizes, the deposits are formed with a shape of a ball segment (this fact gives us grounds to expect this shape for deposits resulting from evaporating microdroplets). As the particle concentration increases, the sphericity of a deposit is distorted and its shape acquires signs of a torus. This indicates that the concentration of particles in macrodroplets of the dispersions at the final stage of evaporation substantially differs from that corresponding to their dense packing.

5. EFFECT OF SOLVENT COMPOSITION

It seems quite reasonable to control the structure of a deposit via the composition of a dispersion medium. Indeed, variations in its composition cause variations in the contact angle, which governs almost all processes relevant to droplet evaporation [23–27], as well as the evaporation rate itself [19]. In this study, we performed experiments with polystyrene dispersions having particle diameter d_p = 540 nm and a concentration of 1 wt %, while aqueous DMSO solutions were used as dispersion media. The concentrations of the used solutions and corresponding contact angles of droplets on a polystyrene film are listed in Table 4 (for the hydrophilic substrate, the contact angle was 30° and varied with the solvent composition within the data scatter observed upon droplet application). The density of DMSO (1.1 g/cm^3) is close to the density of water, while its surface tension is 43.7 mJ/m^2.

In the experiments, 280-pL microdroplets of a colloidal solution of microspheres were applied with the

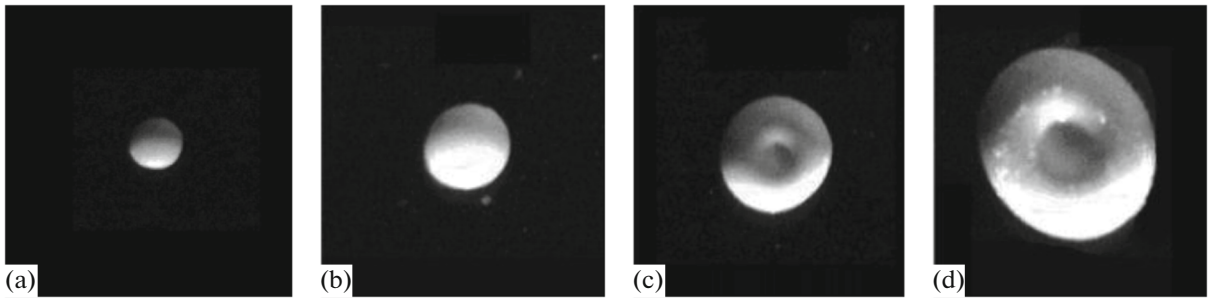

Fig. 8. Optical photographs of deposits formed on a hydrophobic substrate from macrodroplets of polystyrene dispersions with particle concentrations of (a) 0.25, (b) 1.0, (c) 2.5, and (d) 10.0 wt %.

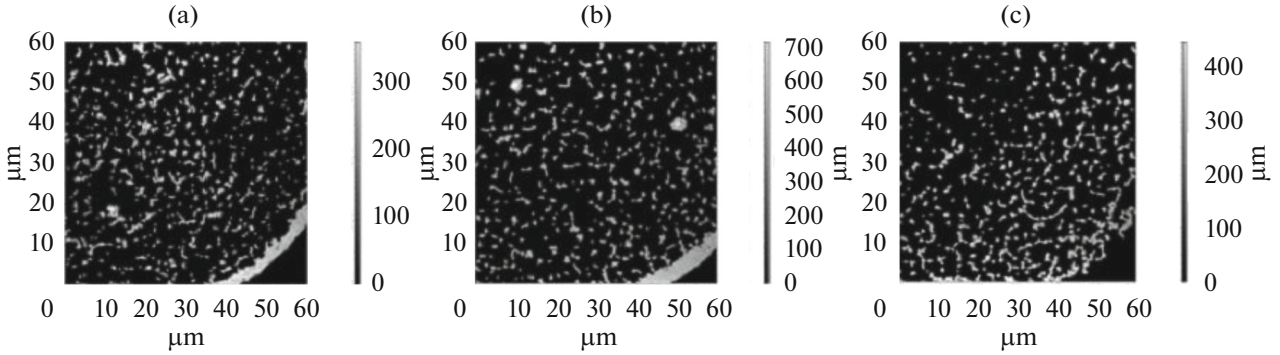

Fig. 9. Structures of ring-shaped deposits formed on a hydrophilic substrate after evaporating microdroplets of dispersions with DMSO concentrations of (a) 0, (b) 20, and (c) 66 wt % (AFM data).

Jetlab II setup onto CGs (hydrophilic surface) and CGs coated with polystyrene layers (hydrophobic surface). Deposits formed on the substrates after dispersion medium evaporation were investigated with optical and atomic force microscopes. Macrodroplets of the same colloidal solution with a volume of 10 μL were applied onto the same hydrophilic and hydrophobic substrates with the dosing pipette. The structures resulting from evaporating macrodroplets were studied on the video stand.

5.1. Hydrophilic Substrate

The sizes of the ring-shaped deposits resulting from evaporating microdroplets are listed in Table 5, while their structures are shown in Fig. 9.

The data in Table 5 and Fig. 9 testify that an increase in the fraction of DMSO in the dispersion medium to 20% has no effect on the diameter and structure of the ring-shaped deposits. A further increase in the DMSO fraction causes a rise in the diameter followed by the disappearance of the ring-shaped deposit itself.

Table 4. Contact angle values for droplets of water/DMSO solutions on polystyrene film

DMSO concentration, wt %	0	5	10	20	33	66
Contact angle, deg	85	85	83	77	70	52

As has been mentioned above, the thickness of the ring is determined by the intensity of compensatory flows. This leads us to state that their intensity decreases with an increase in DMSO concentration probably due to a reduction in the evaporation rate of the dispersion medium and a rise in the role of the diffusion leveling of the particle concentration in the droplet bulk. The growth of the ring size and its final "spreading" seem to be due to the lower value of the solution surface tension and a decrease in the contact angle (see Table 4), as well as the suppression of the transfer of nanoparticles to the meniscus region.

For evaporating macrodroplets, an increase in DMSO concentration has almost no effect on the sizes of ring-shaped deposits (Table 5); however, their heights substantially decrease (Fig. 10). This is caused by the deceleration of the transfer of particles with the compensatory flows, which is also evident from a change in the particle density distribution along the contact spot radius. An analogous decrease in the height of a ring-shaped deposit upon evaporation of dispersion droplets was mentioned in [19]. In some sense, the results obtained for macrodroplets reproduce the regularities found for microdroplets.

Namely: the presence of the second solvent in a concentration below 20 wt % has a weak effect on the structure of a deposit. A further increase in the DMSO concentration causes a reduction in the intensity of the compensatory flows, which leads to a decrease in the height of the peripheral ring and a thickening of the layer of particles deposited inside it. The rise in the thickness of this layer is naturally matched with a decrease in the height of the main ring. Owing to the suppression of the compensatory flows, the transfer of particles to the meniscus slows down, and, at the final stage of droplet evaporation, the particle concentration in it appears to be high.

Table 5. Diameters of ring-shaped deposits as depending on DMSO concentration C_D for micro- and macrodroplets of dispersions evaporating on hydrophilic and hydrophobic substrates

C_D, wt %	0	5	10	20	33	66
Hydrophilic substrate						
d_n, μm	155	147	148	142	178	171
d_m, mm	6.7	6.3	6.7	6.3	6.5	6.6
Hydrophobic substrate						
d_n, μm	55	71	81	143	119	107
d_m, mm	1.6	2.9	3.5	4.2	4.7	5.7

5.2. Hydrophobic Substrate

The characteristics of the deposits resulting from the evaporation of dispersion microdroplets on a hydrophobic substrate are presented in Table 5 and Fig. 11. Recall that, in this case, droplets evaporate in the regime "at an unchanged shape," with the wetting line moving until the pinning begins. Then, at rather large radii (at a high content of DMSO), compensatory flows providing the formation of peripheral rings arise. The data presented show an interesting fact of a rise in the spot radius with an increase in the DMSO concentration from 5 to 20 wt % and its decrease with a subsequent growth of DMSO concentration. The radii of the ring-shaped deposits increase due to a reduction in the surface tension, which leads to the earlier pinning. The decrease in the radii may be explained by the fact that, as DMSO concentration increases, the affinity of the substrate to the aqueous solution grows, thereby leading (as in the case of the hydrophilic substrate) to the spreading of the ring, i.e., the deposition of a small amount of particles, to which the meniscus could be strongly anchored. As a result, the evaporation process is accompanied by a reduction in the radius of the droplet/substrate contact spot. The compensatory flows are poorly developed, and the particles are not delivered to the meniscus region. In the long run, sparse regions of deposited particles begin to be formed on the substrate, to which the meniscus begins to be anchored as if a "partial pinning" takes place. The low density of such (accidentally formed) regions results in the star-shaped structure of the ring perimeter. The final pinning leads to the development of compensatory flows and the formation of a rather dense deposit.

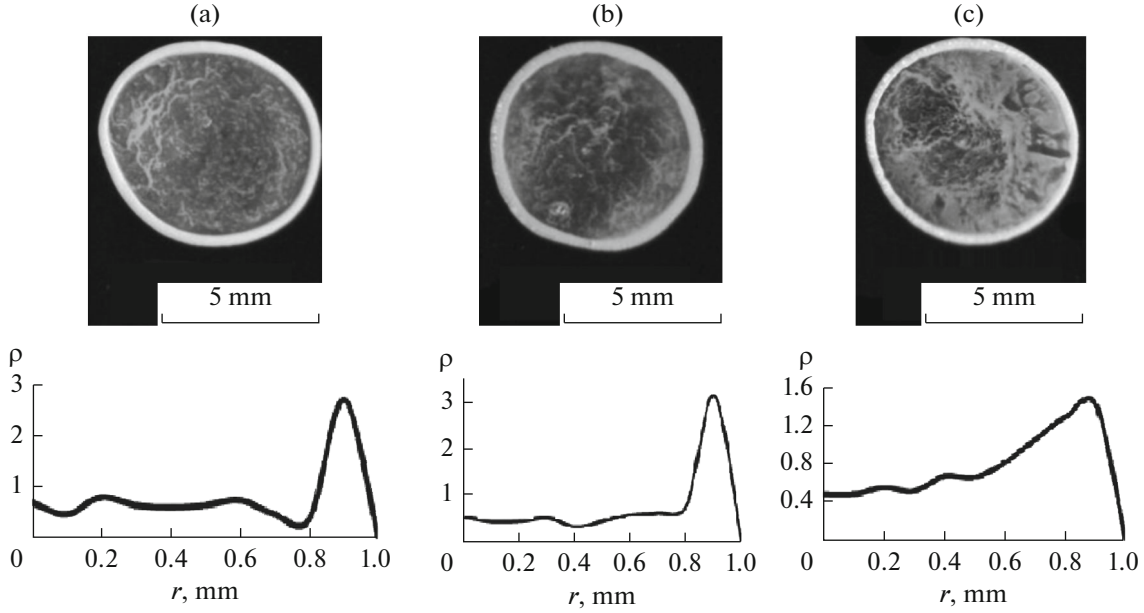

Fig. 10. Optical photographs of ring-shaped deposits formed on a hydrophilic substrate after evaporating macrodroplets of dispersions with DMSO concentrations of (a) 0, (b) 20, and (c) 66 wt % and corresponding radial profiles of particle concentrations ρ (below).

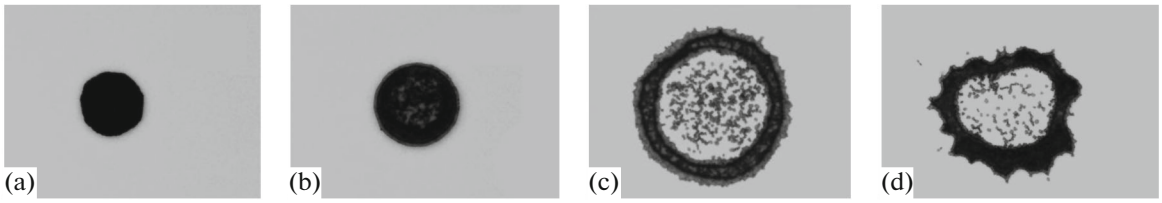

Fig. 11. Structures of deposits formed on a hydrophobic substrate after evaporating microdroplets of dispersions with DMSO concentrations of (a) 0, (b) 5, (c) 20, and (d) 66 wt %.

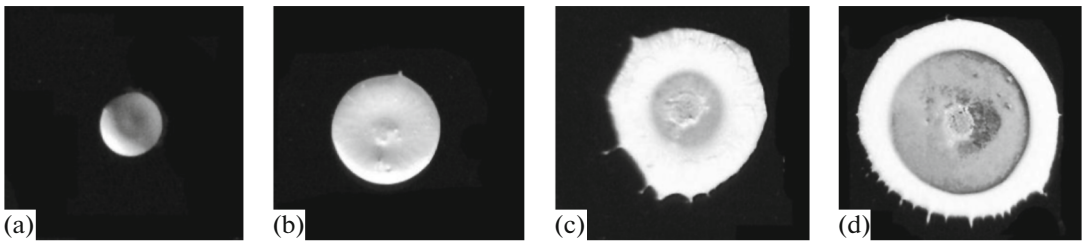

Fig. 12. Structures of deposits formed on a hydrophobic substrate after evaporating macrodroplets of dispersions with DMSO concentrations of (a) 0, (b) 5, (c) 20, and (d) 66 wt %.

In the case of macrodroplets, a decrease in the surface tension of the dispersion medium also leads to a noticeable change in the structure of a formed deposit (Table 5, Fig. 12). In contrast to microdroplets, the ring radius monotonically increases with DMSO concentration. This fact is easily explained by a reduction in the surface tension and an increased affinity of the substrate to the concentrated DMSO solution in water. Under these conditions, pinning may take place at the initial stage of droplet evaporation, thereby leading to the development of compensatory flows and the formation of a pronounced ring-shaped structure. The content of particles in the solution appears to be sufficient (the volume/perimeter ratio is high) for their deposition in an amount providing conditions for pinning during macrodroplet evaporation.

The evaporation of droplets of polystyrene particle dispersions in water/DMSO mixtures comprises one more mechanism of convective motion affecting the formation of the ring-shaped deposit. The Marangoni convection is concerned. Evaporation rates of water and DMSO are different. The faster evaporation of water in the meniscus region leads to the local increase in the DMSO concentration. Its increased concentration causes a stronger decrease in the surface tension. As a result, the surface tension gradient induces a flow, which transfers particles from the meniscus region toward the top of the droplet. As a consequence, the droplet concentration in the meniscus region decreases, and the formation of the ring-shaped deposit slows down. Probably, it is this fact that explains its spreading upon evaporation of solution microdroplets. It is obvious that, in the case of macrodroplets, the Marangoni convection, which affects the surface layer of a droplet, suppresses the contribution of the compensatory flows to a less extent, and the formed deposits have a pronounced ring-shaped structure.

5.3. Formation of Disc-Shaped Deposits

In the previous series of experiments performed with the use of water/DMSO solutions as dispersion media, deposits were obtained having the shape of either a ball segment or a rather narrow ring. It is of practical interest to determine a dispersion medium composition, at which particles would form a disc-shaped structure on a substrate. Such structures may, in particular, be demanded for the jet printing of diverse microcircuits, in which the uniform application of an active medium is preferable. It is a priori obvious that this problem requires the selection of dispersion media with rather complex compositions. It has appeared that it may be solved using three-component solutions.

We shall exemplify this possibility by a dispersion medium consisting of ethanol, which has a high evaporation rate; ethylene glycol, which evaporates slowly and strongly affects the surface tension; and water.

The experiments were performed with dispersions of polystyrene particles 250 nm in diameter. Before applying droplets, dispersions were subjected to ultrasonic treatment (30 min, 40°C). CGs were used as substrates. Droplets were applied onto the substrates using the Jetlab II setup. Droplet images were taken with a video camera supplied with the setup. The deposits resulting from droplet evaporation were studied with an optical microscope.

Table 6. Dispersion medium compositions in two series of experiments on formation of disc-shaped deposits

First series						
C_w, vol %	96.0	94.0	92.0	90.0	88.0	86.0
C_E, vol %	0.0	2.0	4.0	6.0	8.0	10.0
Second series (C_E = 10 vol %)						
C_w, vol %	86.0	76.0	66.0	56.0	46.0	36.0
C_{Et}, vol %	0.0	10.0	20.0	30.0	40.0	50.0

Dispersions of polystyrene particles (concentration of 4%) were prepared in two- and three-component solutions, the compositions of which are listed in Table 6. In the first series of the experiments, two component solvents (water, the concentration of which is denoted as C_w, and ethylene glycol) were used; in the second one, three-component solvents with fixed ethylene glycol content C_E = 10 vol % and variable ethanol concentration C_{Et} were applied.

The experiments have shown that, in the absence of ethanol, ring-shaped structures are formed at any ethylene glycol content (see Fig. 13a). Increasing content of ethanol initially has a weak effect on the deposit structure; however, at its concentration of 50 vol %, the deposit becomes disc-shaped (Fig. 13c).

The performed observations have indicated that, in all experiments of the first series, the deposits have a ring-shaped structure. In the central region, the surface density of particles on the substrate was low, while a pronounced ring (border) was formed along the perimeter. In the second series, the particle concentration in the central region of a contact spot noticeably increased; however, the ring remained preserved, which gradually lost its contrast with a rise in ethanol content, and, at C_{Et} = 50 vol %, a flat disc was actually formed.

It may be assumed that the passage to the disc-shaped structure of the deposit proceeds as follows. The nonuniform evaporation of different components of a dispersion medium continuously occurs in a droplet, with the compensatory flows being suppressed by Marangoni convection. At C_{Et} = 50 vol %, this situation seems to be maintained until water and ethanol are almost completely evaporated. Since ethylene glycol evaporates much more slowly than water and ethanol do, it alone remains in the droplet in the long run. Initial concentration of ethylene glycol is low (10 vol %); therefore, the droplet becomes actually flat at the final stage. Moreover, the low evaporation rate of ethylene glycol implies a low intensity of compensatory flows at this stage as well. A uniform deposit of particles is naturally formed on the substrate in this situation.

7. CONCLUSIONS

The performed investigations have shown that deposit structure may be widely varied by altering the characteristics of a colloidal dispersion, the nature of a substrate, and an initial size of an evaporating droplet. The efficiencies of these factors are not equal. Variations in the dispersion medium composition are most efficient. They enable one to obtain both pronouncedly ring-shaped deposits and deposits having the shape of monolithic discs. This is, obviously, due to the fact that variations in the dispersion medium composition affect important parameters such as the contact angle and droplet evaporation rate. As has been mentioned above, these physicochemical parameters are dominant in the CRE. The data presented confirm their most important role as compared with the other characteristics of dispersion droplets.

The evaporation rate may also be varied by altering the temperature of a substrate and an environment. It appeared that variations in the temperature of a system also lead to fundamental transformations in the deposit structure. Therewith, the temperature effect possesses its own specific features, which will be considered in a subsequent communication.

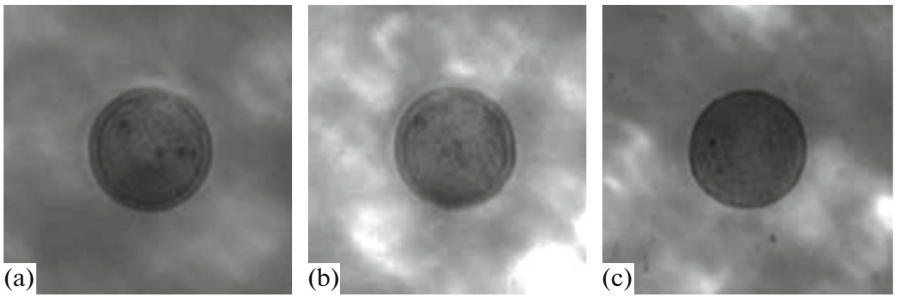

Fig. 13. Structures of deposits formed after evaporating droplets of dispersions with ethanol concentrations C_{Et} = (a) 0, (b) 30, and (c) 50 wol %.

ACKNOWLEDGMENTS

We are grateful to N.A. Chernyshev for his help in the experimental studies. This work was supported by the Russian Foundation for Basic Research (project nos. 16-08-00554a and 15-03-02300a) and the Program of Basic Research of the Presidium of the Russian Academy of Sciences (P1.8)

REFERENCES

1. Roldughin, V.I., *Usp. Khim.*, 2004, vol. 73, p. 123.
2. Terekhin, V.V., Dement'eva, O.V., and Rudoy, V.M., *Usp. Khim.*, 2011, vol. 80, p. 477.
3. Lebedev-Stepanov, P.V., Kadushnikov, R.M., Molchanov, S.P., Ivanov, A.A., Mitrokhin, V.P., Vlasov, K.O., Rubin, N.I., Yurasik, G.A., Nazarov, V.G., and Alfimov, M.V., *Nanotechnol. Russ.*, 2013, vol. 8, nos. 3–4, p. 137.
4. Deegan, R.D., Bakajin, O., Dupont, T.F., Huber, G., Nagel, S.R., and Witten, T.A., *Nature* (London), 1997, vol. 389, p. 827.
5. Deegan, R.D., Bakajin, O., Dupont, T.F., Huber, G., Nagel, S.R., *Phys. Rev. E: Stat. Phys., Plasmas, Fluids, Relat. Interdiscip. Top.*, 2000, vol. 62, p. 756.
6. Bhardwaj, R., Fang, X., Somasundaran, P., Attinger, D., and Witten, T.A., *Langmuir*, 2010, vol. 26, p. 7833.
7. Dugyala, V.R. and Basavaraj, M.G., *Langmuir*, 2014, vol. 30, p. 8680.
8. Yunker, P.J., Still, T., Lohr, M.A., and Yodh, A.G., *Nature* (London), 2011, vol. 476, p. 308.
9. Shen, X., Ho, C.-M., and Wong, T.-S., *J. Phys. Chem. B*, 2010, vol. 114, p. 5269.
10. Li, Y.-F., Sheng, Y.-J., and Tsao, H.-K., *Langmuir*, 2013, vol. 29, p. 7802.
11. Vysotskii, V.V., Roldughin, V.I., Uryupina, O.Ya., and Zaitseva, A.V., *Colloid J.*, 2011, vol. 73, p. 176.
12. Vysotskii, V.V., Uryupina, O.Ya., Senchikhin, I.N., and Roldughin, V.I., *Colloid J.*, 2013, vol. 75, p. 142.
13. Vysotskii, V.V., Uryupina, O.Ya., Senchikhin, I.N., and Roldughin, V.I., *Colloid J.*, 2013, vol. 75, p. 634.
14. Vysotskii, V.V., Roldughin, V.I., Uryupina, O.Ya., Senchikhin, I.N., and Zaitseva, A.V., *Colloid J.*, 2014, vol. 76, p. 531.
15. Nazarov, V.G. and Stolyarov, V.P., *Colloid J.*, 2016, vol. 78, p. 75.
16. Huang, W., Cui, L., Li, J., Luo, C., Zhang, J., Luan, S., Ding, Y., and Han, Y., *Colloid Polym. Sci.*, 2006, vol. 284, p. 366.
17. Sefiane, K. and Bennacer, R., *J. Fluid Mech.*, 2011, vol. 667, p. 260.
18. David, S., Sefiane, K., and Tadrist, L., *Colloids Surf. A*, 2007, vol. 298, p. 108.
19. Vysotskii, V.V., Roldughin, V.I., Uryupina, O.Ya., Senchikhin, I.N., and Zaitseva, A.V., *Colloid J.*, 2015, vol. 77, p. 431.
20. Vysotskii, V.V., Roldughin, V.I., and Uryupina, O.Ya., *Colloid J.*, 2004, vol. 66, p. 777.
21. Wilson, A.S., Brown, E.L., Villa, C., Lynnerup, N., Healey, A., Ceruti, M.C., Reinhard, J., Previgliano, C.H., Araoz, F.A., Diez, J.G., and Taylor, T., *Proc. Natl. Acad. Sci. U. S. A.*, 2013, vol. 110, p. 13322.
22. Chen, R., Zhang, L., Zang, D., and Shen, W., *Adv. Colloid Interface Sci.*, 2016, vol. 231, p. 1.
23. Molchanov, S.P., Roldughin, V.I., and Chernova-Kharaeva, I.A., *Colloid J.*, 2015, vol. 77, p. 761.
24. Molchanov, S.P., Roldughin, V.I., and Chernova-Kharaeva, I.A., *Colloid J.*, 2015, vol. 77, p. 770.
25. Molchanov, S.P., Roldughin, V.I., Chernova-Kharaeva, I.A., and Yurasik, G.A., *Colloid J.*, 2016, vol. 78, p. 633.
26. Molchanov, S.P., Roldughin, V.I., Chernova-Kharaeva, I.A., and Yurasik, G.A., *Colloid J.*, 2017, vol. 79, p. 234.
27. Molchanov, S.P., Roldughin, V.I., Chernova-Kharaeva, I.A., Yurasik, G.A., and Senchikhin, I.N., *Colloid J.*, 2017, vol. 79, p. 515.
28. Men'shikova, A.Yu., Shabsel's, B.M., Evseeva, T.G., Shevchenko, N.N., and Bilibin, A.Yu., *Russ. J. Appl. Chem.,* 2005, vol. 78, p. 159.
29. Stöber, W., Fink, A., and Bohn, E., *J. Colloid Interface Sci.*, 1968, vol. 26, p. 62.
30. Lebedev-Stepanov, P.V., Kadushnikov, R.M., Molchanov, S.P., Rubin, N.I., Shturkin, N.A., and Alfimov, M.V., *Ross. Nanotekhnol.*, 2010, vol. 5, nos. 11–12, p. 83.

Translated by A. Kirilin